JACS
JOURNAL OF THE AMERICAN CHEMICAL SOCIETY

COMMUNICATION

pubs.acs.org/JACS

Fullerene−Carbene Lewis Acid−Base Adducts

Huaping Li,[†] Chad Risko,[‡] Jung Hwa Seo,[§] Casey Campbell,[‡] Guang Wu,[†] Jean-Luc Brédas,[‡] and Guillermo C. Bazan*[,†]

[†]Center for Polymers and Organic Solids, Departments of Chemistry & Biochemistry and Materials, University of California, Santa Barbara, California 93106, United States

[‡]Center for Organic Photonics and Electronics, School of Chemistry and Biochemistry, Georgia Institute of Technology, Atlanta, Georgia 30332-0400, United States

[§]Department of Materials Physics, College of Natural Science, Dong-A University, 840 Hadan 2-dong, Sahagu, Busan 604-714, Republic of Korea

Supporting Information

ABSTRACT: The reaction between a bulky N-heterocyclic carbene (NHC) and C_{60} leads to the formation of a thermally stable zwitterionic Lewis acid−base adduct that is connected via a C−C single bond. Low-energy absorption bands with weak oscillator strengths similar to those of n-doped fullerenes were observed for the product, consistent with a net transfer of electron density to the C_{60} core. Corroborating information was obtained using UV photoelectron spectroscopy, which revealed that the adduct has an ionization potential ∼1.5 eV lower than that of C_{60}. Density functional theory calculations showed that the C−C bond is polarized, with a total charge of +0.84e located on the NHC framework and −0.84e delocalized on the C_{60} cage. The combination of reactivity, characterization, and theoretical studies demonstrates that fullerenes can behave as Lewis acids that react with C-based Lewis bases and that the overall process describes n-doping via C−C bond formation.

From the classic concepts of Gilbert Lewis, one can define a base as a chemical species that utilizes a doubly occupied orbital for promoting a chemical reaction, while an acid corresponds to a species that takes advantage of an empty orbital for initiating a reaction.[1] A prototypical Lewis acid−base (LA/LB) pair can be found in the adduct obtained upon mixing F_3B with $:NH_3$, namely, $F_3B{:}NH_3$ (also denoted as $F_3B{\leftarrow}NH_3$), in which electron density from the amine is transferred to the electron-deficient borane (Scheme 1). Adducts of this type contain what is often called a capto-dative bond and exhibit partial positive charge on nitrogen and partial negative charge on boron. Carbon-based Lewis bases derived from stable N-heterocyclic carbene (NHC) species[2] such as 1,3-di-*tert*-butylimidazolin-2-ylidene (**1** in Scheme 1) have received considerable attention because of their role in the coordination sphere of catalytically active transition-metal organometallic complexes.[3] More recent work has shown that all-carbon compounds can also be described as LA/LB pairs. A specific example is the reaction of NHCs with electron-poor allenes to yield compounds such as **2**.[4] These species are relevant from the perspective of attaining frustrated Lewis pair reactivity, wherein steric hindrance prevents or minimizes the strength of the capto-dative bond and allows for small-molecule activation, such as the heterolytic cleavage of hydrogen.[5] Moreover, all-carbon LA/LB pairs open opportunities for the development of coordination complexes that depart from the normal use of metal ions[6] and heavier elements[7] as the acidic centers.

Scheme 1. (top) Typical LA/LB Pair Formation with F_3B and $:NH_3$ and (bottom) Molecular Structures of N-Heterocyclic Carbene 1 and the LA/LB Product 2 Obtained by Reaction of 1 with an Electron-Poor Allene

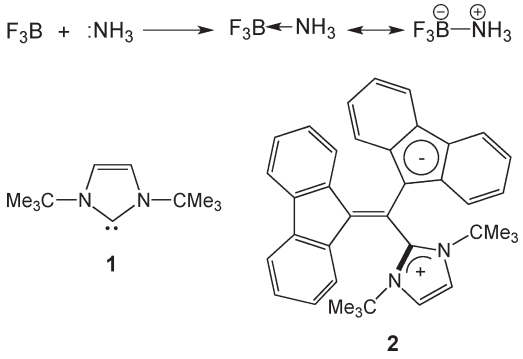

C_{60}, the archetypal fullerene molecule, exhibits an energetically low-lying lowest unoccupied molecular orbital (LUMO).[8] Neutral derivatives have been extensively used in conjunction with suitable conjugated polymers in the fabrication of organic photovoltaic solar cells,[9] where photoinduced electron-transfer reactions from the polymer to the fullerene are the essential processes whereby charge carriers are generated in these devices.[10] The large electron affinity and threefold-degenerate LUMO of C_{60} also allow it to reversibly accept up to six electrons when treated using electrochemical methods.[11] Fullerenes can thus be reduced with electropositive metals,[8] and the resulting fulleride products can exhibit a range of electrical properties, including superconductivity in the case of certain alkali-metal salts.[12]

Herein we show that the simple reaction between the NHC 1,3-bis(diisopropylphenyl)imidazol-2-ylene[13] (**IDipp** in Scheme 2) and C_{60} yields an unexpected C−C-bonded product (**IDipp**−C_{60}) that can be described as an LA/LB adduct, is characterized by a strong zwitterionic character, and displays near-IR (NIR) absorption profiles similar to those of n-doped fullerides.[14] Density functional

Received: May 30, 2011
Published: July 17, 2011

Scheme 2. The Reaction of IDipp and C_{60} in *o*-DCB Yields IDipp−C_{60} [Ar = 2,6-$((CH_3)_2CH)_2C_6H_3$]

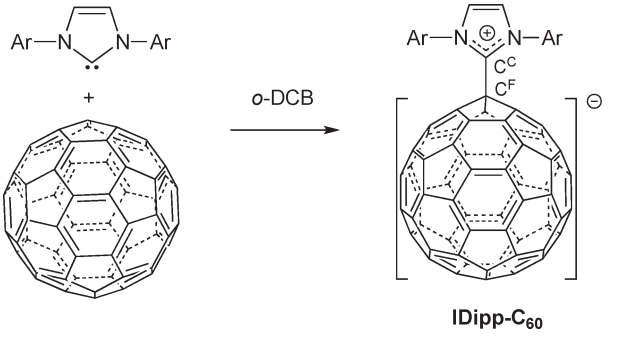

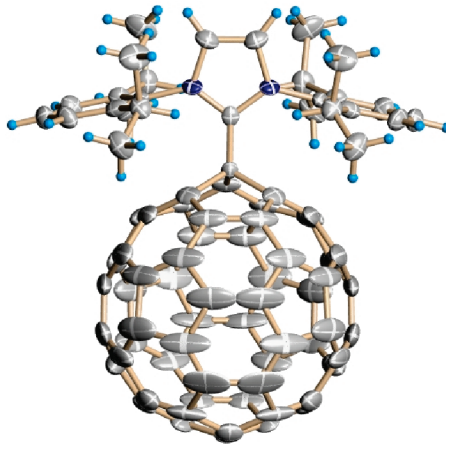

Figure 1. ORTEP drawing of **IDipp**−C_{60} with thermal ellipsoids at the 50% probability level, as determined from X-ray crystallography (carbon, gray; nitrogen, blue; hydrogen, cyan).

theory (DFT) calculations were carried out to provide corroborating evidence of the charge distribution, bonding characteristics, and electronic properties of **IDipp**−C_{60}. The reaction of C_{70} and **IDipp** provides a similar adduct, suggesting that this type of reaction is general.

In a typical reaction, equivalent molar quantities of C_{60} and **IDipp** were dissolved in *o*-dichlorobenzene (*o*-DCB) and allowed to react at room temperature for 24 h. After purification by washing with toluene and tetrahydrofuran, single crystals of the dark-colored product suitable for X-ray diffraction studies were obtained in *o*-DCB at 298 K. The molecular structure was determined and refined on the basis of the space group $P21/m$ for a data set obtained at 160 K, and the results are shown in Figure 1 [for crystal data and structure refinement details, see Table S1 in the Supporting Information (SI)]. Strikingly, one observes that the product corresponds to the simple σ adduct between the two starting materials. The length of the C^C−C^F bond connecting the two fragments [1.502(16) Å] is consistent with single-bond character. Additionally, the visible protrusion of C^F argues against the presence of a hidden H atom at an adjacent position. On the basis of these data, we propose that the reaction between C_{60} and **IDipp** provides **IDipp**−C_{60} as shown in Scheme 2. These results contrast with previously observed reactivity with smaller carbenes, which yield cyclopropane species.[15,16]

The nature of the bonding was more precisely delineated via DFT optimization of **IDipp**−C_{60} (C_s symmetry) using the B3LYP functional[17−19] and a 6-31G** basis set. Natural bond order (NBO) analysis confirmed that the bridging C−C bond (1.54 Å) between the fullerene (C^F) and carbene (C^C) is a σ single bond (Wiberg bond index = 0.97), with an electron occupancy of 1.97e. The hybrid composition of the σ single bond is σ_{CC} = $0.693C^F(sp^{3.41})$ + $0.721C^C(sp^{1.44})$, where C^F has 22.6% s and 77.3% p character while C^C has 41.0% s and 59.0% p character; a pictorial representation of the natural bond orbital is shown in Figure 2a. The sp^3 character of C^F described by the NBO analysis further confirmed the interpretation derived from the X-ray crystallographic data. The DFT results also indicated a considerable dipole moment (μ_{total} = 15.2 D) pointing in a direction aligned with the C^F−C^C bond and that the C^F−C^C bond itself is fairly polarized, with C^F and C^C having charges of −0.13*e* and +0.55*e*, respectively. Total charges of +0.84*e* and −0.84*e* reside on the **IDipp** framework and the fullerene, respectively; the negative charge is spread throughout the fullerene core, although as one might expect a priori, C^F and a few neighboring carbon atoms hold a significant portion (~55%) of the negative charge. The overall picture of the charge distribution corresponds well with a substantial transfer of electron density from the carbene to the fullerene and the zwitterionic nature depicted in Scheme 2. It is also worth highlighting that two potential reaction products, the [5,6]-open and [6,6]-closed cyclopropane analogues of **IDipp**−C_{60}, were evaluated at the B3LYP/6-31G** level of theory (see the SI) and found to be energetically less favorable by 1.50 eV (34.6 kcal/mol) and 1.05 eV (24.1 kcal/mol), respectively, relative to **IDipp**−C_{60}.

Solution characterization methods were used to confirm **IDipp**−C_{60} as the major product in Scheme 2. After the crude product was washed with solvents, its ^{1}H NMR spectrum displayed chemical shifts at 7.51 (s, 2H), 7.22 (t, 2H), 7.10 (d, 4H), 3.27 (sept, 4H), 1.20 (d, 12 H), and 1.15 (d, 12 H) ppm (Figure S1 in the SI); these correspond to the H atoms of **IDipp**. The ^{13}C NMR spectrum (Figure S2) exhibited signals of the isopropyl

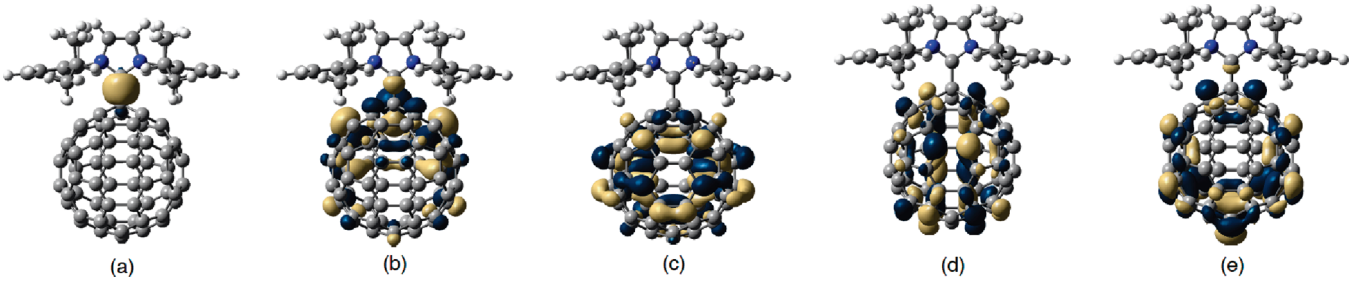

Figure 2. (a) Natural bond orbital for the C^F−C^C σ bond of **IDipp**−C_{60}. (b) HOMO, (c) LUMO, (d) LUMO+1, and (e) LUMO+2 for **IDipp**−C_{60}, as determined at the B3LYP/6-31G** level.

dx.doi.org/10.1021/ja204974m |*J. Am. Chem. Soc.* 2011, 133, 12410–12413

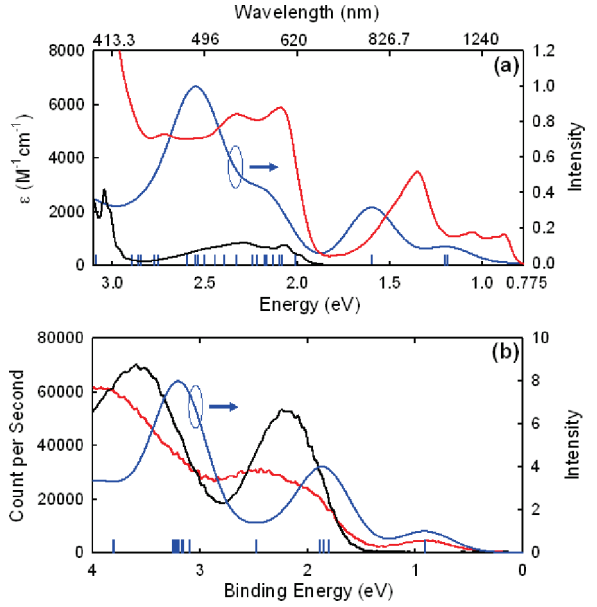

Figure 3. (a) Vis−NIR absorption spectra of C_{60} (black) and **IDipp−C$_{60}$** (red) and a simulated vis−NIR absorption profile for **IDipp−C$_{60}$** (blue) determined using TDDFT at the B3LYP/6-31G** level. The vertical bars show the singlet excited-state energies. (b) UPS spectra of **IDipp−C$_{60}$** (red) and C_{60} (black) films atop a freshly evaporated gold surface and the simulated electron DOS for **IDipp−C$_{60}$** (blue) determined at the B3LYP/6-31G** level. The vertical bars refer to the populations of electronic states.

fragments at 30.1, 26.1, and 21.4 ppm. There were 37 other ^{13}C signals between 120 and 160 ppm, assigned to 30 sp^2 carbons of C_{60} and six carbons for **IDipp**, reflecting C_s symmetry. A signal at 60.7 ppm was assigned to the sp^3 carbon in the C_{60} core. The results of electrospray ionization/time-of-flight mass spectrometry (Figure S3) and elemental analysis were also in agreement with the formation of **IDipp−C$_{60}$**.

A comparison of the UV−vis−NIR spectra of C_{60} and **IDipp−C$_{60}$** in *o*-DCB is shown in Figure 3a. Most significantly, one observes that adduct formation leads to the appearance of bands with weak molar absorption coefficients (ε) in the 800−1600 nm (0.78−1.55 eV) region: 1416 nm (0.88 eV, ε =1155 M^{-1} cm^{-1}), 1178 nm (1.05 eV, ε =1250 M^{-1} cm^{-1}), and 921 nm (1.35 eV, ε =3480 M^{-1} cm^{-1}). It is worth noting at this point that anionic C_{60} displays similar low-energy absorption bands with an onset at ∼1140 nm.[14]

Figure 3a also shows a simulated vis−NIR absorption profile of **IDipp−C$_{60}$** as determined using time-dependent DFT (TD-DFT) calculations at the B3LYP/6-31G** level. There is good agreement in regard to the overall shape of the absorption profiles, with the calculated peaks consistently blue-shifted by ∼0.3 eV with respect to experiment (a feature consistent with expectations for the level of theory employed).[20,21] The first peak in the absorption profile, which is of weak intensity, comprises two near-degenerate transitions at 1.19 eV (1046 nm) and 1.20 eV (1033 nm) that are one-electron excitations from the highest-occupied molecular orbital (HOMO) to the LUMO (99%) and the LUMO+1 (99%), respectively. This peak is followed by a second, slightly more intense one at 1.60 eV (777 nm) due to the HOMO → LUMO+2 (98%) one-electron excitation. The high-energy absorption peaks arise from a series of transitions of weak-to-moderate oscillator strength between 2.0 and 3.4 eV.

Table 1. Frontier MO Energies (in eV) As Determined by DFT at the B3LYP/6-31G Level**

	HOMO-1	HOMO	LUMO
IDipp−C$_{60}$[a]	−5.09	−4.19	−2.43
C_{60}[b]	−7.31	−5.99	−3.23
Δ_{HOMO}[c]		−1.80	

[a] The HOMO is nondegenerate, while the LUMO/LUMO+1, HOMO−1/HOMO−2, and HOMO−3/HOMO−4 pairs are nearly degenerate. [b] The HOMO is fivefold-degenerate, the HOMO−1 fourfold-degenerate, and the LUMO threefold-degenerate. [c] $\Delta_{HOMO} = E_{HOMO}(C_{60}) - E_{HOMO}$(**IDipp−C$_{60}$**). From the UPS data, $\Delta^{exptl}_{HOMO} = -1.5$ eV.

UV photoelectron spectroscopy (UPS) was used to examine differences in the occupied electronic states of **IDipp−C$_{60}$** and C_{60}. A typical experiment involved spin-casting a ∼5 mg/mL *o*-DCB solution atop a freshly evaporated gold surface to produce a film with a nominal thickness of 5−10 nm. Figure 3b shows the resulting spectra referenced to the Fermi level of the gold underlayer (4.8 eV)[22] (see Figure S4 for the full UPS spectra). Ionization potentials (IPs) were determined from the incident photon energy (21.2 eV), the maximum binding energies (E_b^{max}), and the minimum binding energies (E_b^{min}) according to the equation IP = 21.2 eV − ($E_b^{max} - E_b^{min}$). The solid-state IP of C_{60} was found to be 6.0 eV, which is consistent with previous reports.[23,24] In the case of **IDipp−C$_{60}$**, the lowest binding energy is ∼1.5 eV lower than that of C_{60}; by also taking into account the second lowest peak, one determines that the first and second IPs are 4.5 and 5.5 eV, respectively. Interestingly, the IP decrease in the adduct relative to C_{60} is consistent with that seen in gas-phase UPS of the C_{60} anion.[25] The IP of **IDipp−C$_{60}$** is therefore considerably destabilized relative to that of C_{60}, consistent with the net transfer of electron density.

Figure 2b−e depicts the canonical HOMO, LUMO, LUMO+1, and LUMO+2 of **IDipp−C$_{60}$**.[26] The MOs reside mainly on the fullerene portion of the adduct, but there is a notable difference with respect to their spatial locations. Much of the HOMO is located near the top of the fullerene adjacent to the **IDipp** fragment, with some density residing on C^C. In contrast, the LUMO, LUMO+1, and LUMO+2 (with some density on C^C) are more centrally located on the fullerene. Table 1 provides a summary of the relevant MO energies. Figure 3b shows the simulated electron density of states (DOS) for **IDipp−C$_{60}$**;[27] in terms of the relative shape and peak positions, the DOS reproduces the UPS data well. The UPS spectra indicate that the difference in the first IPs of the two compounds (which is approximately equal to −1 times the difference in the HOMO energies according to Koopmans' theorem)[28] is ∼1.5 eV, while the difference in HOMO energies of the two species is −1.8 eV (Table 1). Overall, there is excellent agreement between the theoretical and experimental results, providing further emphasis of the simple molecular description and charge-transfer characteristics shown in Scheme 1.

Fullerene−NHC carbene adduct formation was extended to C_{70}. Specifically, **IDipp** reacted with C_{70} in *o*-DCB to yield singly bonded **IDipp−C$_{70}$**, in which the **IDipp** fragment is regioselectively connected to a carbon at one pole of C_{70}. A single crystal of the **IDipp−C$_{70}$** product suitable for crystallographic studies was obtained by slowly evaporating its chloroform solution. The resulting molecular structure was determined and refined on the basis of the space group *P*21/*n* for a set of data obtained at 160 K,

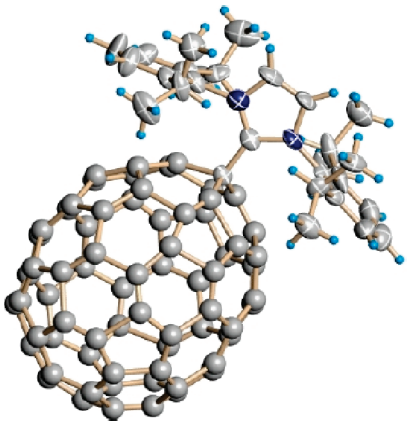

Figure 4. ORTEP drawing of **IDipp**−C_{70} with thermal ellipsoids at the 50% probability level, as determined from X-ray crystallography (carbon, gray; nitrogen, blue; hydrogen, cyan).

and the results are given in Figure 4 (see Table S2 for crystal data and structure refinement details). The ^{1}H NMR profile of **IDipp**−C_{70} differed somewhat from that of **IDipp**−C_{60} (Figure S1). Specifically, chemical shifts appeared at 7.36 (t, 2H), 7.29 (s, 2H), 7.22 (d, 4H), 3.08 (sept, 4H), 1.39 (d, 12 H), and 1.10 (d, 12 H) ppm. This difference suggests that the protons in the **IDipp** substructure experience different shielding, possibly because of the lower symmetry of C_{70}. The successful preparation of **IDipp**−C_{70} indicates that the reactivity described in Scheme 2 is general. Moreover, like **IDipp**−C_{60}, **IDipp**−C_{70} shows low-energy absorption features (Figure S5), indicating a similar type of electronic description for the two molecular entities.

From the simple chemical synthesis, molecular structure, and electronic characteristics of the **IDipp**−C_{60} zwitterion, one learns that it is possible to use fullerenes as Lewis acids that bind to stable carbene bases. Steric bulk surrounding the NHC functionality and delocalization of the positive charge near C^C likely play an important role in avoiding cyclopropane formation, which occurs in the case of smaller carbenes and silyl carbenes. From a materials perspective, the overall process is akin to n-doping of a semiconducting organic molecule via C−C bond formation, but the transfer of electron density is not as complete as that obtained using an electropositive metal. **IDipp**−C_{60} thus provides an unexpected connection between emerging perspectives on all-carbon LA/LB compounds and efforts to control the electrical and magnetic properties of organic semiconductors.

■ ASSOCIATED CONTENT

Supporting Information. Experimental details, vis−NIR absorption, NMR, and mass spectra, and crystal data (CIF) and structure refinement details. This material is available free of charge via the Internet at http://pubs.acs.org.

■ AUTHOR INFORMATION

Corresponding Author
bazan@chem.ucsb.edu

■ ACKNOWLEDGMENT

The research at UCSB was supported by the National Science Foundation (DMR-1035480) and the Department of Energy through the Center of Energy Efficient Materials. The work at Georgia Tech was partly supported by the STC Program of the National Science Foundation (DMR-012967) and by the Center for Advanced Molecular Photovoltaics (CAMP) through Award KUS-C1-015-21 from King Abdullah University of Science and Technology (KAUST).

■ REFERENCES

(1) Jensen, W. B. *Chem. Rev.* **1978**, *78*, 1.
(2) Arduengo, A. J. *Acc. Chem. Res.* **1999**, *32*, 913.
(3) Herrmann, W. A. *Angew. Chem., Int. Ed.* **2002**, *41*, 1290.
(4) Inés, B.; Holle, S.; Goddard, R.; Alcarazo, M. *Angew. Chem., Int. Ed.* **2010**, *49*, 8389.
(5) Welch, G. C.; Juan, R. R. S.; Masuda, J. D.; Stephan, D. W. *Science* **2006**, *231*, 1124.
(6) Hahn, F. E.; Jahnke, M. C. *Angew. Chem., Int. Ed.* **2008**, *47*, 3122.
(7) Back, O.; Donnadieu, B.; Parameswaran, P.; Frenking, G.; Bertrand, G. *Nat. Chem.* **2010**, *2*, 369.
(8) Hirsch, A.; Brettreich, M. *Fullerenes: Chemistry and Reactions*; Wiley-VCH: Weinheim, Germany, 2005.
(9) Yu, G.; Gao, J.; Hemmelen, J. C.; Wudl, F.; Heeger, A. J. *Science* **1995**, *270*, 1789.
(10) Sariciftci, N. S.; Smilowtz, L.; Heeger, A. J.; Wudl, F. *Science* **1992**, *258*, 1474.
(11) Echegoyen, L.; Echegoyen, L. E. *Acc. Chem. Res.* **1998**, *31*, 593.
(12) Ganin, A. Y.; Takabayashi, Y.; Jeglic, P.; Arcon, D.; Potocnik, A.; Baker, P. J.; Ohishi, Y.; McDonald, M. T.; Tzirakis, M. D.; McLennan, A.; Darling, G. R.; Takata, M.; Rosseinsky, M. J.; Prassides, K. *Nature* **2010**, *466*, 221.
(13) Arduengo, A. J., III; Krafczyk, R.; Schmutzler, R. *Tetrahedron* **1999**, *55*, 14523.
(14) Reed, C. A.; Bolskar, R. D. *Chem. Rev.* **2000**, *100*, 1075.
(15) Nikawa, H.; Nakahodo, T.; Tsuchiya, T.; Wakahara, T.; Rahman, G. M. A.; Akasaka, T.; Maeda, Y.; Liu, M. T. H.; Meguro, A.; Kyushin, S.; Matsumoto, H.; Mizorogi, N.; Nagase, S. *Angew. Chem., Int. Ed.* **2005**, *44*, 7567.
(16) Win, W. W.; Kao, M.; Eiermann, M.; McNamara, J. J.; Wudl, F.; Pole, D. L.; Kassam, K.; Warkentin, J. *J. Org. Chem.* **1994**, *59*, 5871.
(17) Becke, A. D. *Phys. Rev. A* **1988**, *38*, 3098.
(18) Becke, A. D. *J. Chem. Phys.* **1993**, *98*, 5648.
(19) Lee, C.; Yang, W.; Parr, R. G. *Phys. Rev. B* **1988**, *37*, 785.
(20) Silva-Junior, M. R.; Schreiber, M.; Sauer, S. P. A.; Thiel, W. *J. Chem. Phys.* **2008**, *129*, No. 104103.
(21) Jacquemin, D.; Perpète, E. A.; Ciofini, I.; Adamo, C.; Valero, R.; Zhao, Y.; Truhlar, D. G. *J. Chem. Theory Comput.* **2010**, *6*, 2071.
(22) de Boer, B.; Hadipour, A.; Mandoc, M. M.; van Woudenbergh, T.; Blom, P. W. M. *Adv. Mater.* **2005**, *17*, 621.
(23) Benning, P. J.; Martins, J. L.; Weaver, J. H.; Chibante, L. P. F.; Smalley, R. E. *Science* **1991**, *252*, 1417.
(24) Maxwell, A. J.; Brühwiler, P. A.; Nilsson, A.; Mårtensson, N.; Rudolf, P. *Phys. Rev. B* **1994**, *49*, 10717.
(25) Yang, S. H.; Pettiette, C. L.; Conceicao, J.; Cheshnovsky, O.; Smalley, R. E. *Chem. Phys. Lett.* **1987**, *139*, 233.
(26) C_{60} was also evaluated at the B3LYP/6-31G** level.
(27) To account for polarization effects in the solid state, the DOS was rigidly shifted with respect to the binding energy axis; contraction/expansion of the simulated curves was not taken into account for the simulated DOS.
(28) Koopmans, T. *Physica* **1934**, *1*, 104.